# Polymer parallel optical waveguide with graded-index rectangular cores and its dispersion analysis

**Tomoya Kosugi and Takaaki Ishigure**

*Faculty of Science and Technology, Keio University, 3-14-1 Hiyoshi, Kohoku-ku, Yokohama, 223-8522, Japan*
*ishigure@appi.keio.ac.jp*

**Abstract:** A low-loss and high-bandwidth polymer parallel optical waveguide with graded-index (GI) rectangular cores is fabricated for high-speed and high-dense optical interconnections. We demonstrate that the near-parabolic index profile formed in the rectangular-shaped core GI waveguide exhibits superior properties similar to those of GI circular core waveguides we previously reported. In particular, we focus on the modal dispersion in the GI polymer waveguides with rectangular cores by showing experimental results. In this paper, the GI rectangular cores are fabricated using the preform method. However, conventional photo-lithography and imprinting processes are viable to fabricate a similar waveguiding structure, by which fabrication of a printed circuit board embedding this waveguide would become feasible.



**OCIS codes:** (200.4650) Optical interconnects; (230.7370) Waveguides; (250.5460) Polymer waveguides

## References and links

1. C. Berger, B. J. Offrein, and M. Schmatz, "Challenges for the introduction of board-level optical interconnect technology into product development roadmaps," Proc. SPIE **6124**, 61240J1–12 (2006)
2. K. Nakano, R. Kuribayashi, K. Maeda, A. Noda, J. Sakaki, and H. Takahashi, "Development of alicyclic polymers for multimode waveguide array and its characteristics for use in optical interconnection," in *proceedings of IEEE Conference on Polymers and Adhesives in Microelectronics and Photonics* (National Museum of Emerging Science and Innovation in Tokyo, Japan, 2007), pp. 170–173.
3. H. Tsushima, E. Watanabe, S. Yoshimatsu, S. Okamoto, T. Oka, and K. Imoto, "Novel manufacturing process of waveguide using selective photobleaching of polysilane films by UV light irradiation," Proc. SPIE **5246**, 119–130 (2003).
4. T. Ishigure, and Y. Takeyoshi, "Polymer waveguide with 4-channel graded-index circular cores for parallel optical interconnects," Opt. Express **15**(9), 5843–5850 (2007).
5. Y. Takeyoshi, K. Matsumoto, and T. Ishigure, "Low-loss 4 x 2 channels polymer optical waveguide with circular graded-index cores for high-density integration on printed circuit boards," in *proceedings of IEEE conference on Electronic Components and Technology Conference* (Lake Buena Vista, Florida, 2008), pp. 2111–2116.
6. Y. Koike, Y. Takezawa, and Y. Ohtsuka, "New interfacial copolymerization technique for steric GRIN polymer optical waveguides and lens arrays," Appl. Opt. **27**(3), 486–491 (1988).
7. S. Eguchi, H. Asano, A. Kannke, and M. Ibamoto, "Gradient index polymer optical waveguide patterned by ultraviolet irradiation," Jpn. J. Appl. Phys. **28**(Part 2, No. 12), L2232–L2235 (1989).
8. R. T. Chen, "Graded index linear and curved polymer channel waveguide arrays for massively parallel optical interconnects," Appl. Phys. Lett. **61**(19), 2278–2280 (1992).
9. M. Karppinen, T. Alajoki, A. Tanskanen, K. Kataja, J.-T. Mäkinen, K. Kautio, P. Karioja, M. Immonen, and J. Kivilahti, "Parallel optical interconnect between ceramic BGA packages on FR4 board using embedded waveguides and passive optical alignments," in *proceedings of IEEE conference on Electronic Components and Technology Conference* (San Diego, California, 2006), pp. 779–805.
10. R. Dangel, C. Berger, R. Beyeler, L. Dellmann, M. Gmür, R. Hamelin, F. Horst, T. Lamprecht, T. Morf, S. Oggioni, M. Spreafico, and B. J. Offrein, "Polymer-waveguide-based board-level optical interconnect technology for datacom applications," IEEE Trans. Adv. Packag. **31**(4), 759–767 (2008).
11. T. Kosugi, and T. Ishigure, "Multimode parallel polymer optical waveguide with graded-index rectangular cores for optical interconnects," in *proceedings of IEEE Conference on Opto-Electronics and Communications Conference, and the Australian Conference on Optical Fibre Technology* (Sydney, Australia, 2008)
12. Y. Takeyoshi and T. Ishigure, "High-density 2 x 4-channel polymer optical waveguide with graded-index circular cores," J. Lightwave Technol. (to be published)

#113536 - $15.00 USD  Received 29 Jun 2009; revised 17 Aug 2009; accepted 17 Aug 2009; published 24 Aug 2009

13. T. Ishigure, M. Satoh, O. Takanashi, E. Nihei, T. Nyu, S. Yamazaki, and Y. Koike, "Formation of the refractive index profile in the graded index polymer optical fiber for gigabit data transmission," J. Lightwave Technol. **15**(11), 2095–2100 (1997).
14. Y. Koike, T. Ishigure, and E. Nihei, "High-bandwidth graded-index polymer optical fiber," J. Lightwave Technol. **13**(7), 1475–1489 (1995).
15. R. Olshansky, and D. B. Keck, "Pulse broadening in graded index optical fibers," Appl. Opt. **15**(2), 483–491 (1976).
16. T. Ishigure, K. Ohdoko, Y. Ishiyama, and Y. Koike, "Mode coupling control and new index profile of GI POF for restricted launch condition in very short-reach networks," J. Lightwave Technol. **23**(12), 2445–2448 (2005).
17. T. Ishigure, S. Tanaka, E. Kobayashi, and Y. Koike, "Accurate refractive index profiling in a graded-index plastic optical fiber exceeding gigabit transmission rates," J. Lightwave Technol. **20**(8), 1449–1456 (2002).

## 1. Introduction

In high performance computers (HPCs) and core routers in data communication networks, the required data throughput has been growing explosively. In such equipment, interconnections in backplanes and on-board are the bottleneck in the total data throughput, since electrical interconnects are still utilized in them. To overcome the limitations of data throughput, optical interconnects have been advantageous.

Specifically, multimode polymer optical waveguides have been drawing much attention because of low material and processing costs with high productivity; polymer parallel multimode waveguides are also one of the feasible solutions for off-chip interconnections. Thus, various polymer waveguides have been proposed, so far [1–3]. In the case of the on-board interconnections, several centimeters of waveguides would be used, because of which lithography or imprinting processes have been widely adopted for polymer waveguides. Therefore, the refractive index of the cores in those waveguides is uniform (step-index (SI) profile). In the SI waveguides, all the modes propagate by total internal reflection, which can cause scattering loss at the rough core-cladding boundary. Moreover, coupling of the scattered light signals to adjacent cores, which is called crosstalk, would be another concern.

In order to address these issues, we have focused on polymer optical waveguides with graded-index (GI) cores [4,5]. As far as we know, there have recently been few reports since several were published in the late 1980's [6,7] which discuss "GI-core polymer optical waveguides." The main application of the GI polymer waveguides reported almost 20 years ago would be optical couplers or lens arrays. Therefore, the diameters of the cores were mostly on the order of millimeters and thus, the high density alignment of multiple GI cores with tens of microns inter-core pitch have not been realized. On the other hand, a single-mode polymer waveguide with graded-index was also demonstrated in the early 1990's [8], but the index profile formed seems asymmetric in the core. Recently, we demonstrated a multimode parallel polymer waveguide with symmetric parabolic index cores with a diameter of 50 μm and similar order of pitch for the application of high-density board-level optical interconnections. These new waveguides are fabricated by means of the heat-drawing process of a preform [4]. The multiple small "circular" GI cores in those waveguides realize excellent transmission properties, for instance, low propagation loss, high-bandwidth and low inter-channel crosstalk. We confirmed that such remarkable characteristics of the novel waveguide were achieved by confining the light around the core center due to the GI profile.

Although the polymer waveguides with GI circular cores showed excellent properties as well, the integration of the waveguides on a printed circuit broad (PCB) would be a key issue, since the GI waveguides are fabricated by the preform method, and obtained independently from PCBs, as shown in Fig. 1. For board-level optical interconnection applications, lots of research have been carried out on waveguide embedded PCBs [9,10], most of which utilize photolithographic processes for fabrication as indicated in Fig. 1.

Given these design considerations, in this paper, we propose a new polymer parallel optical waveguide with GI "rectangular" cores, as shown in Fig. 1. As illustrated in the left figure in Fig. 1, rectangular-shaped cores are easily fabricated by means of conventional waveguide fabrication methods such as photolithography and imprinting (soft lithography) processes. However as far as we know, there have been few reports that realized polymer optical waveguides with the parabolic index profiles in square or rectangular cores densely

#113536 - $15.00 USD Received 29 Jun 2009; revised 17 Aug 2009; accepted 17 Aug 2009; published 24 Aug 2009

aligned, except for our previous conference paper [11]. Therefore, in this paper, we demonstrate that the near-parabolic index profiles formed in the rectangular cores exhibit superior properties similar to the waveguides with GI circular cores we previously reported.

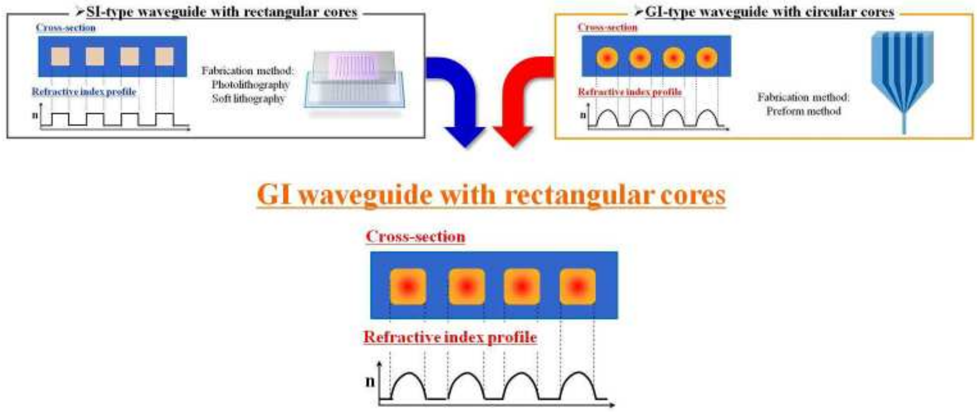


Fig. 1. Schematic concept of our new waveguide.

## 2. Waveguide fabrication

It is preferable to fabricate the new waveguides using lithography or imprinting processes for the on-board applications. On the other hand, in this paper, we adopted the preform method in order to be able to compare the properties of rectangular cores with those of circular counterpart. Actually, we have already succeeded in fabricating the high-quality waveguides with GI circular cores by the preform method [12]. In addition, the preform method is well known as a fabrication method for GI polymer optical fibers (GI-POFs), which is described in more detail in [13,14].

For composing the waveguide, poly methyl methacrylate (PMMA) was used, and dopant with a refractive index higher than that of PMMA was added in the core region in order to form the GI refractive index profile. The rectangular shaped cores are formed by creating a cladding plate that has holes with rectangular cross-sections, as shown in the left figure of Fig. 2. Subsequently, the holes are filled with monomer and dopant (diphenyl sulphide: DPS). The mechanism of forming the index profiles is described in [13,14]. The waveguides are obtained by heat-drawing the preform as shown in Fig. 2, and thus, various kinds of waveguides with desired core size and pitch can be obtained by adjusting the preform design and heat-drawing conditions. Figure 3 (a) shows a cross-section of representative waveguide with four circular cores aligned parallel compared to the one with approximately 100 x 100 μm rectangular (almost square) cores (Fig. 3 (b)) and 60 x 60 μm rectangular cores (Fig. 3 (c)).

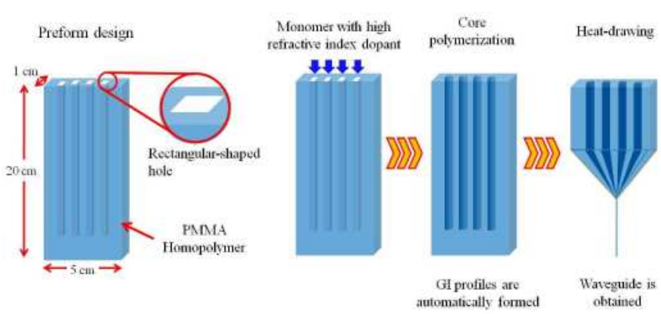


Fig. 2. Schematic representation of fabrication processes

#113536 - $15.00 USD Received 29 Jun 2009; revised 17 Aug 2009; accepted 17 Aug 2009; published 24 Aug 2009

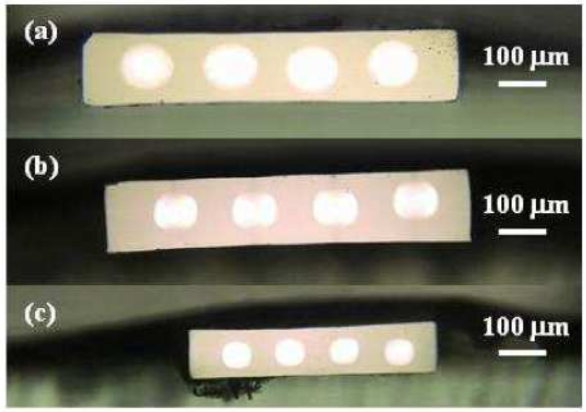


Fig. 3. Cross sections of the 4-channel GI type waveguide with (a) circular cores, (b) 100 x 100 μm rectangular cores and (c) 60 x 60 μm rectangular cores

## 3. Experimental results and discussion

### *3.1 Interference fringe pattern and refractive index profile*

Refractive index profiles of the novel waveguides were measured by a transmitted dual-beam interference microscope (Mizojiri OPTICAL Co., Ltd.). Figure 4 ((a) and (b)) shows the interference fringe patterns of the waveguide measured on the cross-section of a slab sample. Contour patterns of the interference fringes shown in Fig. 4 ((a) and (b)) indicate that the refractive index distributions in the cores are nearly parabolic. It is noted in the square-core waveguide (Fig. 4 (b)) that an almost parabolic index profile is observed from the concentric circular fringe patterns near the core center, which is similar to that in the circular GI core waveguide (Fig. 4 (a)) [4]. Meanwhile, the square-core waveguide shows unique interference fringe patterns: the core center region has circular concentric patterns while square shaped patterns are observed near the core-cladding boundary. Since the optical field of the propagating modes in GI core waveguides is confined near the core center, as we already demonstrated [4], we expect that the difference of the outer core shape (whether circular or square) to have negligible effect on the waveguide properties.

The refractive index profiles is accurately calculated for the first time in our rectangular core waveguides from the fringe patterns as shown in Fig. 4 ((a) and (b)) are shown 2-dimensionally in Fig. 4 (c), (d), and 3-dimensionally in (e), (f). Despite the unique fringe pattern in Fig. 4 (b), the refractive index profile of the new waveguide can be described by the power-law profile similar to circular GI cores. The index profile in the rectangular core is discussed in detail in section 3.4.

By utilizing the interfacial-gel polymerization process, we confirmed that near parabolic (GI) profiles are formed in rectangular-shaped core regions. Moreover, the near parabolic profile compensates the group delay difference among the propagating modes. We mention the modal dispersion of the waveguides in more detail in sections 3.4 and 3.5.

#113536 - $15.00 USD  Received 29 Jun 2009; revised 17 Aug 2009; accepted 17 Aug 2009; published 24 Aug 2009

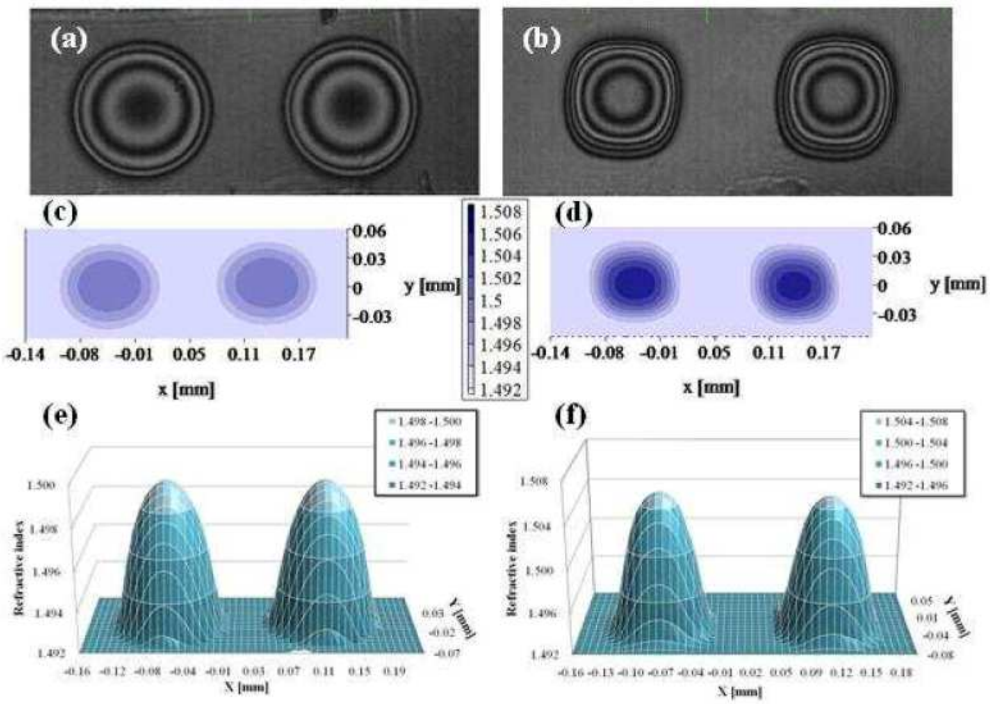


Fig. 4. Interference fringe pattern of the GI waveguide with (a)circular, and (b)rectangular cores Calculated refractive index profile are displayed 2-dimensionally for (c) circular, (d)rectangular cores, and 3-dimensionally for (e) circular, and (f) rectangular cores

### *3.2 Light confinement*

One of the important properties of GI waveguides is strong confinement of the optical field in the core. Figure 5 represents the power distribution at the output ends from (a): 1-m single-mode silica fiber, (b): 5-cm GI rectangular core with a core size of 100 x 100 μm, (c): 1-m GI rectangular core with a core size of 100 x 100 μm, and (d): 5-cm SI rectangular core with a core size of 40 x 40 μm. The broken line in Fig. 5 (b) (c) and (d) signifies the core-cladding boundary. Here, the output power distributions from both polymer waveguides (Fig. 5 (b), (c) and (d) are measured by coupling the output light from the single-mode fiber shown in Fig. 5 (a) directly on the center of the cores of waveguides. It is clearly shown that the output power distribution from the GI square core waveguide is concentrated in the area less than 40 x 40 μm (comparable to SI core waveguide in Fig. 5 (d)). Thus, the optical fields in the GI waveguides are confined near the core center, independent of the outer core shape, as shown in Fig. 5 (b) and (c). On the contrary, the optical field in the SI waveguide is extended to its entire core region, and the output power is uniform over the core region, as shown in Fig. 5 (d).

#113536 - $15.00 USD Received 29 Jun 2009; revised 17 Aug 2009; accepted 17 Aug 2009; published 24 Aug 2009

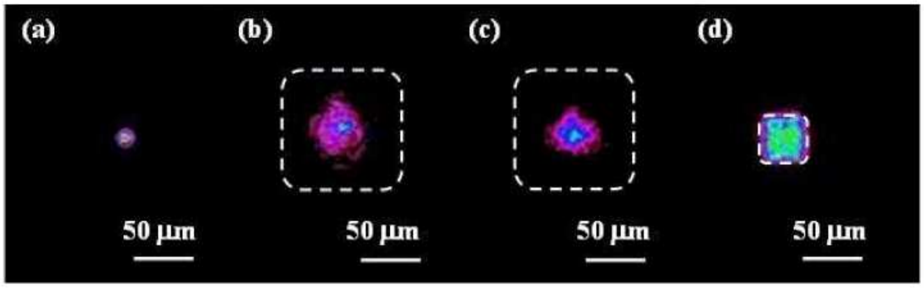


Fig. 5. Experimental results of power distribution at the output ends of (a): 1-m single-mode silica fiber, (b): 5-cm GI rectangular core (100 x 100 μm), (c): 5-m GI rectangular core (100 x 100 μm), and (d): 5-cm SI rectangular core (40 x 40 μm).

While the optical waveguides are utilized in such a short distance, the propagation loss is important, because the loss strongly affects the power budget of the link.

We measured the propagation loss by using the cut-back method, and the propagation loss of the GI waveguide with circular cores and square cores are 0.029 dB/cm and 0.030 dB/cm at 850-nm wavelength, respectively. Compared to existing SI waveguides which have a loss of approximately 0.1 dB/cm on average, very low loss is observed in the GI waveguide. The strong light confinement allows such a low propagation loss less than 0.1 dB/cm, because the scattering loss at the rough core-cladding boundary could be dramatically reduced due to the GI-profile. Thus, the GI waveguide structures inherently have the low transmission loss.

### *3.3 Transmission Capacity for High-Speed Interconnects*

In order to evaluate the performance in actual transmission systems, an eye diagram is measured experimentally after transmitting 12.5 Gbps signal through one core of the 3-m GI waveguides (rectangular-shaped core), as shown in Fig. 6. The wavelength of the signal is 850 nm (California Scientific Inc., V-126). No degradation in the eye diagrams is observed in the GI waveguide even after a 3-m transmission due to small modal dispersion and low propagation loss. Despite the different outer core shape, the new GI waveguides have sufficiently high transmission performance. Although even in SI type waveguides, modal dispersion is not necessarily a serious problem for 10 Gbps transmission for such a short distance as 1 m, the small modal dispersion in the GI waveguide is advantageous for allowing a large power margin and for a large scalability to a link at 20 Gbps and beyond.

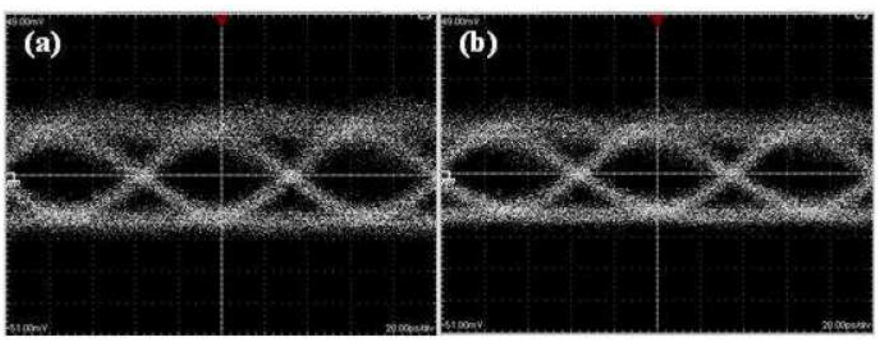


Fig. 6. Eye diagram after a 12.5 Gbps (a):Back-to-Back, (b): 3-m transmission through a rectangular GI core

### *3.4 Bandwidth*

In theoretical modal dispersion analyses, refractive index profiles have generally been approximated by the power-law form by which circularly symmetric index profiles have been mainly discussed [15]. In the case of circular symmetric core, optimum index exponent which

#113536 - $15.00 USD Received 29 Jun 2009; revised 17 Aug 2009; accepted 17 Aug 2009; published 24 Aug 2009

minimizes the total dispersion could be calculated. On the other hand, refractive index profile formed in square or rectangular cores as shown in this paper would be difficult to be expressed by the same power-law form shown by Eq. (1).

$$n(r) = n_1 \left[ 1 - 2\Delta \left( \frac{r}{a} \right)^g \right]^{\frac{1}{2}} \qquad 0 \le r \le a$$
$$= n_2 \qquad r \ge a \qquad (1)$$

Here, $n_1$ is the refractive index of the core, $a$ is the core radius, the parameter $g$, which is called the index exponent, determines the refractive index profile over the region of $0 \le r \le a$, $\Delta$ is defined as:

$$\Delta = \frac{n_1^2 - n_2^2}{2n_1^2}, \qquad (2)$$

where, $n_2$ is the refractive index of the cladding.

Therefore, modal dispersion of square and rectangular core waveguides could be different from those of circular core waveguides. In this section, we focus on the dispersion property of one channel in GI parallel optical waveguides in more detail. For the analysis of modal dispersion (particularly launch condition dependence), it is preferable to use waveguides with a larger core (twice or three times larger than the core size shown in Fig. 5) and long transmission length. For this investigation, GI square-core waveguides (single core) were fabricated and their bandwidth was measured after propagating a length of 90-m. We have also tried to analyze the similar modal properties on parallel polymer optical waveguides, and obtained similar results to those of single core. However, because of the core size, it was very easy to evaluate the characteristics on the single core waveguide compared to parallel core counterpart, particularly in alignment with probe fibers.

The refractive index profiles of the waveguide are shown in Fig. 7. It is also possible to approximate the index profile formed in the square core waveguide by the power-law form if the refractive index profile is defined as a function of the distance $r$ from the core center. However, it could be difficult to determine the unique index exponent $g$ in the power-law form, because the distance between the core center and core edge is different depending on the direction (e.g. diagonal or lateral directions) However, it is very interesting that the index exponent $g$ approximated from the measured profiles shown in Fig. 7 ($g_{\text{horizontal}} = g_{\text{diagonal}} = 4$) coincide, although they were measured in different directions. We fabricated four different samples of square-core waveguides under different core-polymerization conditions, but the index exponents in them show the same tendency. Therefore, we can estimate the optimum index exponent for square or rectangular cores theoretically by defining the index profiles with the unique index exponent value. These results of the theoretical investigation and the index formation mechanism in those square cores will be reported in other articles.

For the bandwidth measurement, we utilized a time-domain measurement method: narrow pulsed optical signals (62.5 ps Full width at half maximum: FWHM) were created by a pulse pattern generator with a semiconductor laser (emitting at a wavelength of 655 nm). The pulsed signals were coupled to the waveguide under two launch conditions: overfilled mode launch (OML) and restricted mode launch (RML) [16]. The output pulse from the waveguide was recorded and analyzed by means of the optical sampling oscilloscope (HAMAMATSU OOS-01)

#113536 - $15.00 USD Received 29 Jun 2009; revised 17 Aug 2009; accepted 17 Aug 2009; published 24 Aug 2009

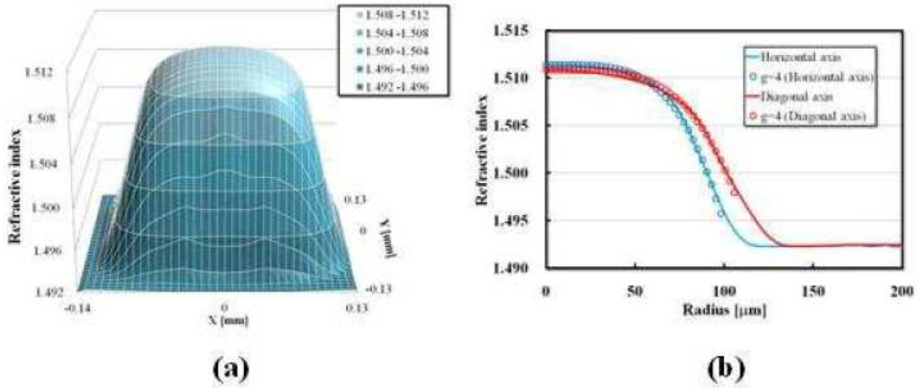


Fig. 7. Refractive index profile of measured GI waveguide (a) and its 2-dimensional profile (b); solid lines are measured profiles and the plots signify the approximated profile by the power-law form

In the case of circular core waveguides with the optimum index profile, the modal dispersion is minimal and a very narrow impulse response function is observed.

On the other hand, Fig. 8 shows the pulse broadening through a 90-m waveguide with a GI square core. Compared to the optimum index exponent for MMA-DPS core in GI POF (circular core) [17], the index exponent of the square core waveguide in Fig. 7 is a little large. Nevertheless, the waveguide with GI square core exhibits very small pulse broadening (impulse response). Actually, the bandwidth obtained by the Fourier transform of the pulse broadening in Fig. 8 is 756 MHz under the OML condition and 1.03 GHz under the RML condition. By investigating the optimum index profile for square cores, theoretically, we expect that bandwidth performance could be greatly improved, which will be described in the other articles.

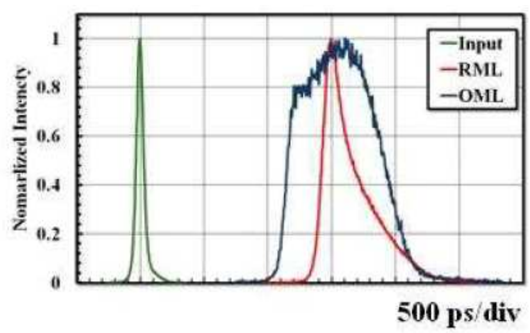


Fig. 8. Output pulse waveforms from a GI square core waveguide under the OML and RML conditions after a 90 m transmission

### *3.5 Group delay*

In order to investigate the difference in the bandwidth between OML and RML in more detail, we adopted differential mode delay (DMD) analysis. Each propagating mode in the waveguide can have different group delay depending on the index profile, and in the case of the DMD analysis, mode coupling (energy transfer among the propagating modes) should be low enough to distinguish the group delay of each mode. For investigating the strength of mode coupling, we generally evaluate the launch condition dependence of NFP. Figure 9 shows the result measured experimentally. Here, the low and high order mode groups are independently launched via a 1-m length SMF probe butt-coupled at the core center and near the core-cladding boundary, respectively. From the GI core waveguide with small mode

#113536 - $15.00 USD Received 29 Jun 2009; revised 17 Aug 2009; accepted 17 Aug 2009; published 24 Aug 2009

coupling, generally, a Gaussian-shaped NFP with a very small spot size is observed for low-order modes, while a ring-like pattern is observed for high-order modes [16]. In Fig. 9, although the difference in the NFPs between low-order and high-order modes is observed, we can confirm that the equilibrium modal distribution is not yet established in this waveguide after a 90-m transmission.

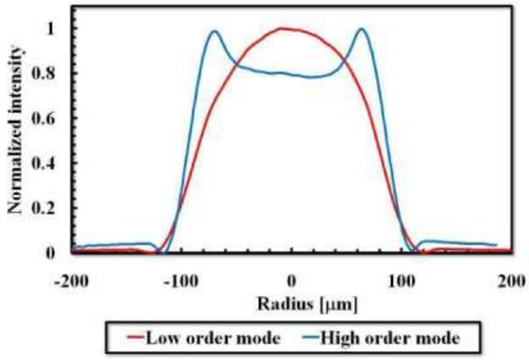


Fig. 9. Comparison of NFP between low order mode and high order mode

In this paper, we employed a streak scope (HAMAMATSU: streak scope C4334) for the DMD measurement. A streak scope is a tool for acquiring the data of time dependent optical intensity (pulse waveform) with respect to the spatial position. By combining the mode order dependence of NFP as indicated in Fig. 9, the group delay of each mode was measured by the streak scope as follows: We used the pulse generator and semiconductor laser same as those for the impulse response function measurement, and all the propagating modes in the waveguides were simultaneously launched via a large-core (1 mm diameter) SI POF probe, as is the aforementioned OML. The output end of the waveguide was coupled to the streak scope to measure the time of flight of the pulsed signal with respect to the spatial position. The group delay was measured after a 90-m (long enough) signal transmission through the same GI square core waveguide as the one for bandwidth measurement in Fig. 8.

The streak images obtained experimentally are shown in Fig. 10. Here, the vertical axis shows the time delay, and the horizontal axis is the spatial position on the cross-section of the waveguide. The inset of Fig. 10 (a) and (b) shows how the waveguide aligned for coupling to the streak scope. The dashed lines in the inset figures correspond to the horizontal axes of Fig. 10 (a) and (b). It is indicated that a large group delay is observed in the high-order modes whose field is located near core-cladding boundary. It is found that the group delay of all the modes are not compensated completely by the GI profile, and that the refractive index profile of this waveguide is of the under-compensated type, as estimated from the index profile. Therefore, the pulse broadening under the OML condition shown in Fig. 8 and the degradation of bandwidth are mainly derived from the group delay of high-order modes.

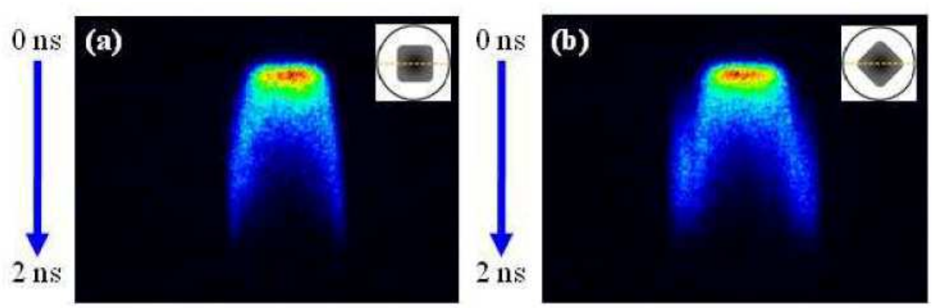


Fig. 10. Streak image of the novel waveguide on horizontal direction (a) and on diagonal direction (b).

#113536 - $15.00 USD Received 29 Jun 2009; revised 17 Aug 2009; accepted 17 Aug 2009; published 24 Aug 2009

Figure 11 represents the group delay of a small mode group with respect to the distance from the core center. The distance is normalized with the length between the core center and the edge of the core. Here, we selected two directions: one is in diagonal and the other is lateral (horizontal), as shown in Fig. 11. In the novel waveguide, the group delay observed within 60% of the distance from the core center is small enough in both the horizontal and diagonal axes. These properties are also found in some waveguides with a GI circular core.

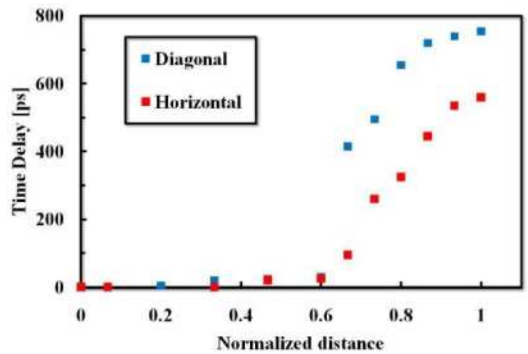


Fig. 11. Comparison of bandwidth between OML and RML condition

In practice, it is expected that polymer parallel waveguides for optical interconnection are used in combination with vertical cavity surface emitting laser (VCSEL) arrays operated at a wavelength of 850-nm. If this waveguide is launched with a VCSEL array, the near RML condition would be realized, because VCSELs have small beam spot-sizes. Therefore, despite the specific modal dispersion of the GI square core as shown in Fig. 11, the tolerance in coupling between VCSELs and cores is sufficiently large.

## 4. Conclusion

We proposed a novel polymer optical waveguide in which graded index profiles are formed in rectangular shaped cores. Then, we demonstrated its high transmission performance.

The novel waveguides have almost identical characteristics to the waveguides with GI circular cores, whereas the interference fringe pattern observed indicates that the refractive index profile is very distinct.

Using the streak scope, it is observed that higher-order modes whose fields mainly exist near the core-cladding boundary have a remarkably large time delay. However, even in the GI rectangular core waveguide, significant modal dispersion reduction is achieved by the GI profile as well as that in waveguides with GI circular core. Therefore, even the near-parabolic index profile formed in the rectangular cores exhibit much higher bandwidth than the conventional SI profile.

These square- or rectangular-shaped cores are expected to be fabricated using conventional photo-lithography and imprinting processes. Thus, we conclude that the novel waveguide with a GI rectangular core is a promising candidate for short-reach optical interconnection applications.

#113536 - $15.00 USD Received 29 Jun 2009; revised 17 Aug 2009; accepted 17 Aug 2009; published 24 Aug 2009